Dosimetric Analysis of Radioimmunotherapy with ^{186}Re-Labeled Bivatuzumab in Patients with Head and Neck Cancer

Ernst J. Postema, MD[1]; Pontus K.E. Börjesson, MD[2]; Wilhelmina C.A.M. Buijs, PhD[1]; Jan C. Roos, MD, PhD[3]; Henri A.M. Marres, MD, PhD[4]; Otto C. Boerman, PhD[1]; Remco de Bree, MD, PhD[2]; Margreet Lang, PhD[5]; Gerd Munzert, MD[6]; Guus A.M.S. van Dongen, PhD[2]; and Wim J.G. Oyen, MD, PhD[1]

[1]Department of Nuclear Medicine, University Medical Center Nijmegen, Nijmegen, The Netherlands; [2]Department of Otolaryngology/Head and Neck Surgery, VU University Medical Center, Amsterdam, The Netherlands; [3]Department of Nuclear Medicine, VU University Medical Center, Amsterdam, The Netherlands; [4]Department of Otolaryngology/Head and Neck Surgery, University Medical Center Nijmegen, Nijmegen, The Netherlands; [5]Boehringer Ingelheim BV, Alkmaar, The Netherlands; and [6]Boehringer Ingelheim Pharma GmbH & Co KG, Biberach an der Riss, Germany

From December 1999 until July 2001, a phase I dose escalation study was performed with ^{186}Re-labeled bivatuzumab, a humanized monoclonal antibody against CD44v6, on patients with inoperable recurrent or metastatic head and neck cancer. The aim of the trial was to assess the safety and tolerability of intravenously administered ^{186}Re-bivatuzumab and to determine the maximum tolerated dose (MTD) of ^{186}Re-bivatuzumab. The data were also used for dosimetric analysis of the treated patients. Dosimetry is used to estimate the absorbed doses by nontarget organs, as well as by tumors. It can also help to explain toxicity that is observed and to predict organs at risk because of the therapy given. **Methods:** Whole-body scintigraphy was used to draw regions around sites or organs of interest. Residence times in these organs and sites were calculated and entered into the MIRDOSE3 program, to obtain absorbed doses in all target organs except for red marrow. The red marrow dose was calculated using a blood-derived method. Twenty-one studies on 18 patients, 5 female and 16 male, were used for dosimetry. **Results:** The mean red marrow doses were 0.49 ± 0.03 mGy/MBq for men and 0.64 ± 0.03 mGy/MBq for women. The normal organ with the highest absorbed dose appeared to be the kidney (mean dose, 1.61 ± 0.75 mGy/MBq in men and 2.15 ± 0.95 mGy/MBq in women; maximum kidney dose in all patients, 11 Gy), but the doses absorbed are not expected to lead to renal toxicity. Other organs with doses exceeding 0.5 mGy/MBq were the lungs, the spleen, the heart, the liver, the bones, and the testes. The doses delivered to the tumor, recalculated to the MTD level of 1.85 GBq/m^2, ranged from 3.8 to 76.4 Gy, with a median of 12.4 Gy. A good correlation was found between platelet and white blood cell counts and the administered amount of activity per kilogram of body weight ($r = -0.79$). **Conclusion:** Dosimetric analysis of the data revealed that the range of doses to normal organs seems to be well within acceptable and safe limits. Tumor doses ranged from 4 to 76 Gy. Given the acceptable tumor doses, ^{186}Re-labeled bivatuzumab could be a good candidate for future adjuvant radioimmunotherapy in patients with minimal residual disease.

Key Words: radioimmunotherapy; dosimetry; head and neck cancer; ^{186}Re-bivatuzumab; monoclonal antibody

J Nucl Med 2003; 44:1690–1699

Squamous cell carcinoma (SCC) is the predominant histologic type among tumors of the head and neck. They account for approximately 5% of all malignant neoplasms in Europe and the United States. Worldwide, more than 500,000 new cases were diagnosed in 2000 (*1*). Patients with early stages of disease (stage I or II) are usually treated with surgery or radiotherapy and have a good prognosis. Patients with stage III or IV disease usually undergo combined surgery and radiotherapy, but the failure rate is high: Locoregional disease recurs after conventional therapy in about 40% of these patients, and distant metastases develop in nearly 25%. The management of these advanced stages of disease especially leaves room for improvement. Development of an effective systemic adjuvant therapy for eradication of minimal residual disease is a major challenge. The use of radiolabeled monoclonal antibodies (mAbs) for this purpose may be a promising approach, since SCC of the head and neck (HNSCC) is a radiosensitive tumor type.

The use of radiolabeled mAbs for the treatment of malignancies is called radioimmunotherapy (RIT). RIT appeared to be a successful treatment modality in patients with non-Hodgkin's lymphoma, a radiosensitive tumor type (*2*). RIT is also used in studies for the treatment of solid tumors. For treatment of HNSCC, the CD44 antigen seems a suitable target. A particular CD44 isoform, containing the variant exon v6 (CD44v6), is expressed homogeneously in almost all tumors derived from squamous epithelium,

Received Mar. 14, 2003; revision accepted Jun. 13, 2003.

For correspondence or reprints contact: Ernst J. Postema, MD, Department of Nuclear Medicine (565), UMC Nijmegen, P.O. Box 9101, 6500 HB Nijmegen, The Netherlands.

E-mail: e.postema@nucmed.umcn.nl

whereas its expression on normal human tissues is highly restricted (*3*). This expression is maintained in tumor metastases, as immunohistochemical evaluation showed homogeneous expression of CD44v6 in 94 of 95 lymph node metastases (*3*). Antibodies directed against CD44v6 were already used in previous clinical RIT trials. In 1998, a phase I study using the ^{186}Re-labeled chimeric mAb U36 was performed for evaluation of the safety and efficacy of RIT (*4*). In 5 of 12 patients treated with U36, human antichimeric antibodies developed. Therefore, a humanized mAb called bivatuzumab, which is also directed against CD44v6, was developed for further clinical trials.

In most RIT trials, the radionuclide ^{131}I or ^{90}Y is used. ^{131}I emits low-energy β-radiation and high-energy, high-abundance γ-radiation. Although, in most cases, treatment with ^{131}I-labeled mAbs can be given on an outpatient basis in the United States (*5*,*6*), the high-energy, high-abundance γ-radiation emitted by ^{131}I may, in some countries, require hospitalization of patients to protect relatives and the general public from radiation. ^{90}Y decays by high-energy β-emissions but lacks γ-radiation. Therefore, scintigraphy and dosimetry cannot be performed when only ^{90}Y-labeled mAbs are used—a limitation, especially when a new mAb is clinically evaluated in RIT for the first time. For this study, ^{186}Re was used because of its excellent physical properties. ^{186}Re decays by both β- and γ-emission. The mean energies of the β-emissions are 362 keV (71% of disintegrations) and 309 keV (22%). The low-energy (137 keV), low-abundance (10%) γ-radiation is ideal for scintigraphy, as shown in Figure 1, and permits treatment on an outpatient basis even at high doses.

Given the encouraging RIT results with ^{186}Re-U36, the ideal physical properties of ^{186}Re, and the availability of a humanized mAb, this study was conducted to assess the safety and tolerability of intravenously administered ^{186}Re-bivatuzumab and to determine the maximum tolerated dose (MTD) of ^{186}Re-bivatuzumab. The data of this trial were also used for dosimetric analysis. Dosimetry can be used to give insight into the radiation doses absorbed by nontarget organs, as well as by tumors. It can also help to explain toxicity that is observed and to predict organs at risk because of the therapy given.

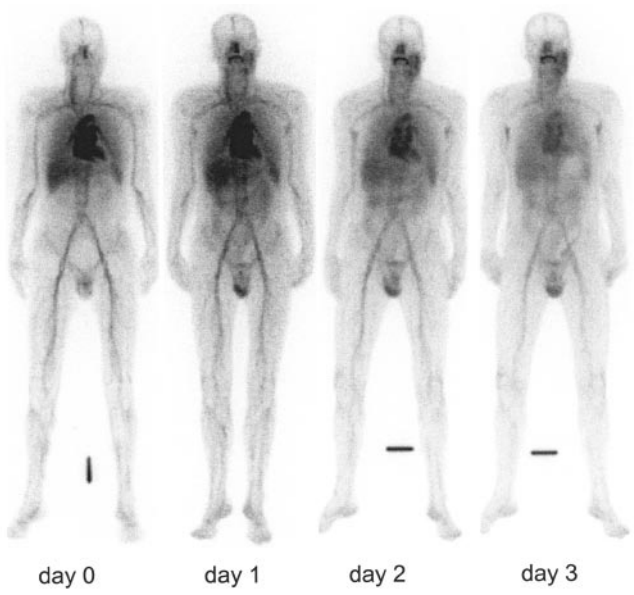

FIGURE 1. Biodistribution directly after and 1, 2, and 3 d after ^{186}Re-bivatuzumab RIT in patient 6, who had carcinoma in the left parotic region.

MATERIALS AND METHODS

Patient Eligibility

Patients with a history of histologically confirmed HNSCC were candidates. At the time they entered the study, they had to have either distant metastases or local or regional recurrent disease for which curative treatment options were not available. The tumor had to be measurable clinically or radiologically. The patients had to be between 18 and 80 y old, give written informed consent, and have a life expectancy of at least 3 mo and a Karnofsky performance status of over 60.

Patients with serious concomitant pathology, such as life-threatening infections, organ failure, or a recent myocardial infarction, were excluded. Other exclusion criteria were allergic diathesis, hematologic disorders, congestive heart failure, unstable angina pectoris, bronchial asthma, pregnancy, or the absence of acceptable means of birth control in fertile women.

The white blood cell (WBC) count had to be at least 3.0×10^9/L, the granulocyte count at least 1.5×10^9/L, and the platelet count at least 100×10^9/L. The last course of chemotherapy or radiotherapy had to have been at least 4 wk before inclusion in the study.

Bivatuzumab

Bivatuzumab (also known as BIWA 4) is a humanized mAb of the IgG1 isotype. It was produced and supplied by Boehringer Ingelheim Pharma GmbH & Co KG. Bivatuzumab recognizes a transmembrane glycoprotein on the outer cell surface. After binding of the mAb to the antigen, an epitope encoded by CD44v6, it is slightly internalized (<20%). This antigen is expressed by all primary head and neck tumors and by the majority of cells within these tumors. In addition, homogeneous expression has been observed in SCC of the lung, skin, esophagus, and cervix (*3*). Heterogeneous expression was found in adenocarcinomas of the breast, lung, colon, pancreas, and stomach (*3*). In normal tissues, expression has been found in epithelial tissues, such as skin, breast, prostate myoepithelium, and bronchial epithelium (*3*). The reactivity of bivatuzumab is essentially restricted to squamous epithelia.

Bivatuzumab was labeled with ^{186}Re using *S*-benzoyl-mercaptoacetyltriglycine (MAG3) as a chelator by the method of Visser et al. (*7*). The radiochemical purity of each ^{186}Re-bivatuzumab batch, as assessed by thin-layer chromatography or high-pressure liquid chromatography, always exceeded 95%. The immunoreactive fraction of each batch ranged from 81% to 100%, with a mean of 90%. ^{186}Re and MAG3 were obtained from Mallinckrodt.

Study Design

The present clinical trial was an uncontrolled dose escalation study. All patients underwent prestudy screening, consisting of a review of their history and physical examination, including

examination by an experienced oncologic ear, nose, and throat surgeon; laboratory analysis; electrocardiography; CT of the thorax; and radiologic assessment of the tumor site by CT, MRI, or ultrasound.

Study treatment consisted of a single injection with 50 mg of bivatuzumab labeled with ^{186}Re in increasing doses, starting at 0.74 GBq/m^2 (20 mCi/m^2), with increments of 0.37 GBq/m^2 (10 mCi/m^2). Two patients were entered at the lowest dose level, at which toxicity did not exceed grade 1 according to the Common Toxicity Criteria, version 2.0, of the National Cancer Institute. At the higher dose levels, 3 patients were entered per level. If dose-limiting toxicity occurred (grade 3 nonhematologic or grade 4 hematologic toxicity), the group treated at that dose level had to be extended to a total of 6 patients. The MTD was defined as the dose level at which not more than 1 of 6 patients experienced dose-limiting toxicity.

Patients who responded to the first treatment with ^{186}Re-bivatuzumab were eligible for a second administration. They underwent the same visit schedule as for the first administration.

Pharmacokinetics

Blood samples for pharmacokinetic analysis were taken directly after injection, at 5 and 30 min after injection, and at 1, 2, 4, 16, 21, 48, 144, 240, and 336 h after injection. Both serum and blood samples were counted in a well-type γ-counter (Wizard 1470 [at the Amsterdam study center] or Wizard 1480 [at the Nijmegen study center]; Wallac) along with standards of the injection solution. The amount of activity in the samples was expressed as percentage injected dose per kilogram of blood or serum.

Scintigraphy

Whole-body scintigrams for visual assessment of biodistribution and for dosimetric analysis were made within 1 h after injection and at 21, 48, 72, and 144 after injection. A known aliquot of the injected dose (gamma camera standard) was inserted in an acrylic block of 15-cm height and was scanned at the same time for reference purposes. At the Nijmegen study center, images were acquired using a Siemens double-head gamma camera. The images were processed at ICON workstations using a locally developed dosimetry tool. This tool allows copying and transferring regions of interest (ROIs) between various whole-body studies. At the Amsterdam study center, the data were acquired with an ADAC double-head gamma camera. Data were transferred electronically in Interfile format and were converted without loss of information to ICON files. These data were analyzed using the same dosimetry tool.

ROIs were drawn around the gamma camera standard; the whole body; the heart and its background; the right lung and its background; the liver; the spleen and its background; the left kidney and its background; the testes, if applicable, and their background; and the tumor, if visible, and its background. All images were reviewed by one physician. The counts in each ROI were corrected for background using the ROIs drawn adjacent to each organ.

Dosimetry

Background Correction. The activity in the body (C_{WB}) was determined as the geometric mean of the counts in the anterior image (CA_{WB}) minus the counts in the standard ROI on the anterior image (CA_{ST}), and the counts in the posterior image (CP_{WB}) minus the counts in the standard ROI on the posterior image (CP_{ST}). This is depicted in Equation 1:

$$C_{WB} = \sqrt{(CA_{WB} - CA_{ST}) \cdot (CP_{WB} - CP_{ST})}. \quad \text{Eq. 1}$$

The activity in the standard (C_{ST}) is determined as the geometric mean of the counts in the ROI on the anterior image (CA_{ST}) and the counts in the ROI on the posterior image (CP_{ST}):

$$C_{ST} = \sqrt{CA_{ST} \cdot CP_{ST}}. \quad \text{Eq. 2}$$

The activity in the heart (C_H) was determined as the geometric mean of the counts in the anterior ROI (CA_H) and in the posterior ROI (CP_H) minus background (Eq. 3). The background in the anterior image ($CA_{H,BG}$) was calculated by multiplying the counts per pixel in the ROI for the background of the heart by the number of pixels in the ROI of the heart. Similarly, the background in the posterior image ($CP_{H,BG}$) was calculated. Partial background subtraction was used: Only a fraction of the counts in the background ROIs was subtracted (*8*). This fraction (*F*) was calculated by dividing abdomen thickness minus organ thickness by the abdomen thickness. For the heart, *F* equals 0.5 (*8*).

$$C_H = \sqrt{(CA_H - 0.5 \cdot CA_{H,BG}) \cdot (CP_H - 0.5 \cdot CP_{H,BG})}. \quad \text{Eq. 3}$$

The activity in the lungs, spleen, and kidneys (C_{ORG}) was determined as the geometric mean of the counts in the anterior ROI (CA_{ORG}) and in the posterior ROI (CP_{ORG}), minus $F = 0.66$ times the background in the anterior image ($CA_{ORG,BG}$) and the posterior image ($CP_{ORG,BG}$), respectively (Eq. 4) (*9*). The background for each organ was calculated similarly to the background for the heart. The activity in the lungs was assumed to be 2 times the activity in the right lung. The activity in the kidneys was assumed to be 2 times the activity in the left kidney.

$$C_{ORG} = \sqrt{(CA_{ORG} - 0.66 \cdot CA_{ORG,BG}) \cdot (CP_{ORG} - 0.66 \cdot CP_{ORG,BG})}. \quad \text{Eq. 4}$$

The activity in the liver (C_{LI}) was determined as the geometric mean of the counts in the anterior ROI (CA_{LI}) and in the posterior ROI (CP_{LI}) (Eq. 5). No background correction was made, since the liver occupies almost the entire thickness of the patient's abdomen (*8*).

$$C_{LI} = \sqrt{CA_{LI} \cdot CP_{LI}}. \quad \text{Eq. 5}$$

The activity in the testes (C_{TE}) was determined using the anterior image only (the geometric mean of the counts in the anterior ROI [CA_{TE}] and the background in the anterior image [$CA_{TE,BG}$]) (Eq. 6).

$$C_{TE} = CA_{TE} - CA_{TE,BG}. \quad \text{Eq. 6}$$

The activity in the tumor (C_T) was determined using either the anterior image (the geometric mean of the counts in the anterior ROI [CA_T] and the background in the anterior image [$CA_{T,BG}$]) or the posterior image (the geometric mean of the counts in the posterior ROI [CA_T] and the background in the posterior image [$CA_{T,BG}$]), depending on the site of the tumor (Eq. 7).

$$C_T = CA_T - CA_{T,BG} \quad \text{or} \quad C_T = CP_T - CP_{T,BG}. \quad \text{Eq. 7}$$

Attenuation Correction. The attenuation of the activity in the whole body and in the abdominal organs was considered to be caused by 11.25 cm of tissue between the center of the patient and the skin. The attenuation of activity in the intrathoracic organs is less, because the lungs contain air, leading to less attenuation.

Therefore, the residence times of these organs are multiplied by 0.85 to correct for the differences in attenuation in the abdomen and thorax.

The residence times of the testes and the tumor are multiplied by 0.25 and 0.58, respectively. The attenuation of the testes by an overlying layer of 1.5 cm of soft tissue can be defined using Equation 8, in which μ equals 0.144 cm^{-1} for 137-keV photons in tissue, and $x = 1.5$ cm of tissue. The attenuation of the abdomen can be defined using the same equation and $x = 11.25$ cm. By dividing $A_{11.25}$ by $A_{1.5}$, a correction factor of 0.25 is obtained.

$$A_x = A_0 \cdot e^{-\mu \cdot x}. \qquad \text{Eq. 8}$$

The distance between the center of the tumor and the skin is thought to be 7.5 cm, leading to a correction factor of 0.58, which is calculated using the same method as described for attenuation correction of the testes.

Residence Times. Equations 1–7 were applied to each imaging time-point to yield time–activity curves for each organ. The activity in the whole body at each time-point was decay corrected. Time–activity curves for the whole body were obtained by assuming no biologic clearance of injected activity at the first imaging time-point. The decay-corrected counts were fit to a single-component exponential clearance expression, yielding the biologic half-life. Assuming that 100% of the injected dose was present at the first imaging time-point, the percentage of the injected dose for each succeeding scan was calculated by dividing counts of each succeeding scan by the counts of the first scan. These data were fit in a single-component exponential clearance expression, yielding the residence time value of the whole body.

Residence times in all organs were calculated using the trapezoidal method. First, a linear extrapolation was made between the assumed uptake fraction of 0 at the time of injection and the measured fractional uptake at the time of the first image. This extrapolation was not corrected for physical decay. From each time-point to the next, a line was drawn between the fractions of uptake. The areas under all these lines were summed. The remaining area under the curve from the end of data collection until infinity was determined by considering only physical decay of the radionuclide.

Absorbed Doses. The absorbed dose to the organs was calculated using the MIRD schema. Tumor, heart (contents), lungs, liver, spleen, kidneys, red marrow, testes, urinary bladder, and the rest of the body (remainder) were considered source organs. The tumor as a source organ was considered to be located at the site of the thyroid gland. Because the organ anatomically nearest to the tumor is the thyroid gland, one cannot estimate the absorbed dose to it. The absorbed dose to the thyroid is expected to be (very) low, since no uptake in the thyroid (and the stomach) is seen, meaning that neither circulation of perrhenate ($^{186}ReO_4^-$) nor actual uptake of radiolabeled antibody occurs in the thyroid. For the bladder, the dynamic bladder model was used. A voiding interval of 4 h was assumed. Using the counts for the whole body, the biologic half-life was determined as described previously. Biologic half-life and voiding interval were entered into the dynamic bladder model, yielding the residence time in the urinary bladder. The calculated residence times as described in the previous section were entered into the MIRDOSE3 computer program, version 3.1 (Oak Ridge Associated Universities) (*10*), to compute the absorbed doses, using the reference adult software phantom for the men. For the women, the adult female phantom was used.

The absorbed doses in the tumors were calculated using the known fraction of activity in the tumor, divided by the weight of the tumor. To assess the volume of the tumor, its 3 dimensions—as assessed by CT scanning—were multiplied by $\pi/6$. The weight was estimated by multiplying the volume of the tumor by its density, being 1.0 g/cm^3. This calculated weight was entered into MIRDOSE3, in which a sphere represents the tumor. The dose rate in each tumor was estimated using iterative approximation.

The red marrow dose (D_{RM}) was estimated using the blood clearance data, as described by Shen et al. (*11*). The absorbed dose in the red marrow (cGy/mCi) is calculated according to Equation 9:

$$D_{RM} = \frac{0.5 \cdot 0.19 \cdot C_{blood}}{1 - Ht} + \frac{0.2128 \cdot \tilde{A}_{WB}}{W_{body}}. \qquad \text{Eq. 9}$$

In Equation 9, Ht represents the patient's hematocrit before infusion (L/L), C_{blood} is calculated using the residence times in blood ($kBq \cdot h \cdot mL^{-1} \cdot MBq^{-1}$), $\tilde{A}_{WB}$ represents the whole-body residence time (h), and W_{body} represents the body weight of the patient (g).

Statistical Analysis

Associations between myelotoxicity and doses were calculated with SPSS 10.0 software (SPSS Inc.) using the Pearson correlation test. Two-sided significance levels were calculated for all parameters, with $P < 0.05$ considered statistically significant.

RESULTS

Twenty patients with locoregional recurrence or metastases of head and neck cancer, and for whom no curative options were available, were included in the trial and treated with ^{186}Re-bivatuzumab. Three of these patients received a second injection with 1.85 GBq/m^2 (50 mCi/m^2) ^{186}Re-bivatuzumab at least 12 wk after the first injection. The specific clinical data of the patients treated and the trial outcome are described elsewhere (*12*). For 2 patients treated, not enough data were available for adequate dosimetric analysis. Thus, the results of the dosimetry of 21 RIT procedures on 18 patients are presented.

Red Marrow Doses

The doses absorbed in the red marrow were estimated for all 21 patient studies, as presented in Table 1. The data of men and women are presented separately, since men and women have different mean blood volumes according to the standard phantom models (5.2 L in men, 3.9 L in women). Therefore, the weight of the bone marrow differs between the sexes, leading to differences in absorbed marrow doses. Table 2 shows the mean absorbed doses at the different dose levels.

Because pharmacokinetic data were used to estimate the red marrow doses, the small variance in absorbed doses suggests a consistency in the pharmacokinetics of these patients.

Absorbed Doses in Other Organs

The calculated residence times in the source organs were entered into the MIRDOSE3 program. The results of the MIRDOSE3 analysis are listed in Tables 3 and 4. Since 2 different models were used (adult and female adult), the

TABLE 1
Absorbed Doses in Red Marrow

Patient no.	Dose level (GBq/m^2)	Dose (GBq)	Red marrow dose (mGy/MBq)	Red marrow dose (Gy)
Men				
1	0.74	1.27	0.522	0.66
3	1.11	2.06	0.503	1.03
4	1.11	1.98	0.532	1.06
6	1.11	2.08	0.511	1.06
7	1.48	2.76	0.497	1.37
8	1.48	2.60	0.524	1.37
10	1.85	3.38	0.459	1.55
11.1	1.85	3.12	0.516	1.61
11.2	1.85	3.17	0.481	1.53
12.1	1.85	3.34	0.486	1.62
12.2	1.85	3.35	0.497	1.67
14.1	2.22	3.83	0.459	1.76
14.2	1.85	3.16	0.438	1.38
15	2.22	4.00	0.481	1.93
18	1.85	3.22	0.514	1.65
19	1.85	3.67	0.449	1.65
Mean ± SD			0.492 ± 0.029	
Women				
2	0.74	1.18	0.635	0.75
9	1.48	2.40	0.622	1.49
13	2.22	3.61	0.624	2.26
16	2.22	3.31	0.619	2.05
20	1.85	2.57	0.684	1.76
Mean ± SD			0.637 ± 0.027	

data for men and women are presented separately. As stated earlier, the thyroid dose could not be estimated. Although MIRDOSE3 lists both the effective dose and the effective dose equivalent, these values are not applicable to patients receiving radiation therapy. As an alternative, the absorbed total-body dose was calculated, considering the body as an organ.

Table 3 shows the mean absorbed doses, expressed as mGy/MBq and grouped by dose level, in all target organs of male patients. The mean dose actually absorbed by all organs was determined by MIRDOSE3 using the reference adult phantom and was calculated by multiplying the mGy/MBq values by the actual dose, in megabecquerels, that the patients received.

The data for the women were processed similarly, using the female adult phantom. The mean absorbed doses, expressed as mGy/MBq, are presented in Table 4. The absorbed doses in women appear to be higher than those in men because of the different reference body weight of the 2 models (female adult, 57 kg; adult, 70 kg). Because the data of only 5 women could be used for dosimetric analysis, no mean absorbed doses per dose level could be given, except for the highest dose level of 2.22 GBq/m^2 (60 mCi/m^2), at which 2 women were treated.

The organ that received the highest doses was the kidney (1.61 ± 0.75 mGy/MBq in men, 2.15 ± 0.95 mGy/MBq in women). Other organs receiving absorbed doses exceeding 0.5 mGy/MBq were the lungs (1.16 ± 0.29 mGy/MBq in men, 1.46 ± 0.22 mGy/MBq in women), the spleen (1.11 ± 0.39 mGy/MBq in men, 1.56 ± 0.53 mGy/MBq in women), the heart (0.83 ± 0.21 mGy/MBq in men, 1.27 ± 0.20 mGy/MBq in women), the liver (0.76 ± 0.17 mGy/MBq in

TABLE 2
Mean Absorbed Doses

Men treated (*n*)	Dose level (GBq/m^2)	Mean absorbed red marrow dose ± SD (Gy)	Women treated (*n*)	Dose level (GBq/m^2)	Mean absorbed red marrow dose ± SD (Gy)
1	0.74	0.66	1	0.74	0.75
3	1.11	1.05 ± 0.02			
2	1.48	1.37 ± 0.00	1	1.48	1.49
8	1.85	1.58 ± 0.09	1	1.85	1.76
2	2.22	1.85 ± 0.12	2	2.22	2.15 ± 0.15

TABLE 3
Absorbed Organ Doses in Men

Organ	Mean absorbed organ dose ± SD (mGy/MBq)	Mean absorbed organ dose for different dose levels ± SD (Gy)				
		0.74 GBq/m² (n = 1)	1.11 GBq/m² (n = 3)	1.48 GBq/m² (n = 2)	1.85 GBq/m² (n = 8)	2.22 GBq/m² (n = 2)
Adrenals	2.08E−01 ± 2.08E−02	0.27	0.44 ± 0.03	0.50 ± 0.09	0.68 ± 0.07	0.89 ± 0.09
Brain	2.01E−01 ± 2.14E−02	0.26	0.42 ± 0.04	0.48 ± 0.09	0.66 ± 0.07	0.86 ± 0.09
Gallbladder wall	2.08E−01 ± 2.11E−02	0.27	0.44 ± 0.04	0.49 ± 0.09	0.68 ± 0.07	0.88 ± 0.09
LLI wall	2.05E−01 ± 2.15E−02	0.27	0.43 ± 0.04	0.49 ± 0.09	0.67 ± 0.07	0.87 ± 0.09
Small intestine	2.05E−01 ± 2.15E−02	0.27	0.43 ± 0.04	0.49 ± 0.09	0.67 ± 0.07	0.88 ± 0.09
Stomach	2.04E−01 ± 2.13E−02	0.27	0.43 ± 0.04	0.49 ± 0.09	0.67 ± 0.07	0.87 ± 0.09
ULI wall	2.05E−01 ± 2.14E−02	0.27	0.43 ± 0.04	0.49 ± 0.09	0.67 ± 0.07	0.88 ± 0.09
Heart wall	8.35E−01 ± 2.12E−01	1.07	1.50 ± 0.10	2.53 ± 0.47	2.78 ± 0.82	3.21 ± 1.09
Kidneys	1.61E+00 ± 7.52E−01	1.80	2.54 ± 1.70	4.20 ± 0.03	6.14 ± 3.06	5.28 ± 2.45
Liver	7.62E−01 ± 1.72E−01	0.60	1.63 ± 0.28	2.39 ± 0.63	2.53 ± 0.48	2.75 ± 0.98
Lungs	1.16E+00 ± 2.89E−01	1.35	2.25 ± 0.77	3.29 ± 0.60	4.00 ± 0.84	3.89 ± 2.20
Muscle	2.02E−01 ± 2.13E−02	0.26	0.43 ± 0.04	0.48 ± 0.09	0.66 ± 0.07	0.86 ± 0.09
Pancreas	2.08E−01 ± 2.11E−02	0.27	0.44 ± 0.04	0.49 ± 0.09	0.68 ± 0.07	0.89 ± 0.09
Bone surfaces	9.22E−01 ± 4.65E−02	1.26	1.96 ± 0.08	2.53 ± 0.06	2.97 ± 0.14	3.51 ± 0.16
Skin	2.00E−01 ± 2.12E−02	0.26	0.42 ± 0.04	0.47 ± 0.09	0.65 ± 0.07	0.85 ± 0.09
Spleen	1.11E+00 ± 3.86E−01	1.97	1.65 ± 0.81	2.67 ± 0.27	3.78 ± 1.35	5.17 ± 0.75
Testes	7.31E−01 ± 2.28E−01	0.65	1.88 ± 0.32	1.77 ± 0.12	2.28 ± 0.81	2.98 ± 1.31
Urinary bladder wall	3.03E−01 ± 3.27E−02	0.37	0.60 ± 0.03	0.85 ± 0.28	1.01 ± 0.09	1.14 ± 0.15
Total body	2.81E−01 ± 1.66E−02	0.36	0.58 ± 0.03	0.71 ± 0.10	0.92 ± 0.05	1.14 ± 0.02

LLI = lower large intestine; ULI = upper large intestine.

men, 1.12 ± 0.26 mGy/MBq in women), the bones (0.92 ± 0.05 mGy/MBq in men, 0.92 ± 0.03 mGy/MBq in women), and the testes (0.73 ± 0.23 mGy/MBq).

Tumor Dosimetry

If CT scanning before treatment with ^{186}Re-bivatuzumab showed a measurable tumor lesion, and if this lesion was visible on scintigraphy after RIT, dosimetry for the tumor was performed. In this study, 15 lesions could be evaluated and were analyzed.

The tumor sizes ranged from 5.1 to 285.9 cm^3. The tumor doses differed markedly: Doses ranged from 1.4 to 73.9 Gy. Because tumor doses in a dose-escalation study cannot easily be compared, tumor doses were calculated postulating that all patients were treated at MTD, being 1.85 GBq/m^2 (50 mCi/m^2). The recalculated tumor doses ranged from 3.8 to 76.4 Gy, with a median dose of 12.4 Gy. The tumor doses of all individual lesions are listed in Table 5.

In the patient studies used for tumor dosimetry, stable disease was observed in 2 cases. The actual absorbed doses in the tumors of these patients were 74 and 16 Gy, respectively.

Correlation Between Toxicity and Absorbed Doses

Because hematologic toxicity appeared to be dose limiting, and because no other serious toxicity was observed, platelet and WBC nadir levels were compared with total injected activity, injected activity per square meter of body surface area, injected activity per kilogram of body weight (all parameters listed in Table 6), whole-body absorbed dose (listed in Tables 3 and 4), and red marrow absorbed dose (as listed in Table 1). Correlation coefficients between nadir of platelets and WBCs, and the 5 parameters mentioned above, were plotted (Fig. 2), calculated, and listed in Table 7. The injected activity per kilogram of body weight appeared to correlate best with hematologic toxicity, with a correlation coefficient of −0.79. Second-best correlations were found between whole-body dose and WBC nadir (r = −0.75) and between administered activity per square meter of body surface area and nadirs (r = −0.73).

DISCUSSION

Dosimetric analysis of patients treated with ^{186}Re-bivatuzumab did not reveal unexpectedly high absorbed doses in normal organs. The organ that received the highest dose is the kidney. Patients treated at MTD and 1 dose level higher (1.85 and 2.22 GBq/m^2, respectively) had absorbed doses in the kidneys of maximally 11 Gy, thus not exceeding 20–25 Gy, a dose that is thought to cause renal toxicity (*13*). Other organs receiving relatively high absorbed doses are the lungs (maximally 5.4 Gy). Because lung toxicity is expected at doses of more than 27 Gy (*14*), the doses found in this trial were thought not to lead to pulmonary problems. For the spleen, the heart, the liver, and the bones, doses were considered to be within safe ranges as well. The absorbed dose in the testes appeared to be maximally 4 Gy, assuming that there was uptake in the testes only and not in the epididymides or scrotal skin. Some uptake in the scrotal skin could be expected, using a radiolabeled antibody that could target skin. In a particular patient, 2 separate testicles

TABLE 4
Absorbed Organ Doses in Women

Organ	Mean absorbed organ dose ± SD (mGy/MBq)	Mean absorbed organ dose for different dosage levels ± SD (Gy)			
		0.74 GBq/m^2 (n = 1)	1.48 GBq/m^2 (n = 1)	1.85 GBq/m^2 (n = 1)	2.22 GBq/m^2 (n = 2)
Adrenals	2.75E−01 ± 3.56E−02	0.37	0.60	0.63	1.00 ± 0.20
Brain	2.66E−01 ± 3.68E−02	0.36	0.57	0.60	0.98 ± 0.21
Breasts	2.66E−01 ± 3.63E−02	0.36	0.57	0.60	0.97 ± 0.20
Gallbladder wall	2.74E−01 ± 3.62E−02	0.37	0.59	0.62	1.00 ± 0.21
LLI wall	2.70E−01 ± 3.70E−02	0.36	0.58	0.61	0.99 ± 0.21
Small intestine	2.70E−01 ± 3.66E−02	0.36	0.58	0.61	0.99 ± 0.21
Stomach	2.71E−01 ± 3.63E−02	0.36	0.58	0.61	0.99 ± 0.21
ULI wall	2.71E−01 ± 3.69E−02	0.36	0.58	0.61	0.99 ± 0.21
Heart wall	1.27E+00 ± 1.97E−01	1.77	3.10	3.57	3.77 ± 0.28
Kidneys	2.15E+00 ± 9.51E−01	1.45	5.69	9.00	6.30 ± 2.58
Liver	1.12E+00 ± 2.59E−01	1.70	2.81	3.24	3.02 ± 0.34
Lungs	1.46E+00 ± 2.17E−01	1.76	3.86	4.37	4.34 ± 0.27
Muscle	2.67E−01 ± 3.66E−02	0.36	0.58	0.60	0.98 ± 0.21
Ovaries	2.70E−01 ± 3.66E−02	0.36	0.58	0.61	0.99 ± 0.21
Pancreas	2.75E−01 ± 3.63E−02	0.37	0.59	0.62	1.00 ± 0.21
Bone surfaces	9.18E−01 ± 2.56E−02	1.10	2.17	2.38	3.18 ± 0.32
Skin	2.64E−01 ± 3.61E−02	0.35	0.57	0.60	0.97 ± 0.20
Spleen	1.56E+00 ± 5.30E−01	1.99	2.09	5.45	5.35 ± 1.70
Urinary bladder wall	3.51E−01 ± 3.91E−02	0.34	0.90	0.92	1.29 ± 0.01
Uterus	2.69E−01 ± 3.66E−02	0.36	0.58	0.61	0.99 ± 0.21
Total body	3.72E−01 ± 2.61E−02	0.48	0.84	0.93	1.30 ± 0.17

LLI = lower large intestine; ULI = upper large intestine.

were seen, thus suggesting that not the scrotum was visualized, but the testes. Relatively high uptake of radiolabeled immunoglobulins in the testes is not unusual. It was also described for patients who received ^{111}In-labeled polyclonal IgG for infection detection (*8*). Few data on the effects of radionuclides on fertility and deterministic effects have been published. Commentary 7 of the National Council on Radiation Protection and Measurements gives a threshold value of 3.5 Gy for external-beam radiation. Because the dose rate of radionuclide therapies is lower when compared with external-beam radiation, doses that can be tolerated by normal organs are higher than doses delivered by external-beam radiation. The effects of RIT on fertility have not been sufficiently established.

TABLE 5
Doses Absorbed by Tumor

Patient no.	Tumor volume (cm^3)	Tumor self-dose S-value (mGy·MBq^{-1}·h^{-1})	Residence time (h)	Administered activity (GBq)	Actual tumor dose (Gy)	Tumor dose if treated at 1.85 GBq/m^2 (Gy)
1	285.9	7.38E−01	1.45	1.27	1.4	3.8
2	11.5	1.79E+01	1.19	1.18	25.2	65.1
3	19.2	1.02E+01	0.32	2.06	6.7	10.8
4	10.8	1.82E+01	0.22	1.98	7.9	13.5
6	11	1.79E+01	0.07	2.08	2.6	4.4
7	47.1	3.84E+00	0.54	2.76	5.7	7.4
8	8.1	2.37E+01	0.11	2.60	6.8	8.7
9	16.2	9.16E+00	0.44	2.40	9.7	12.4
10	5.1	4.14E+01	0.53	3.38	73.9	76.4
13	69.6	2.84E+00	2.65	3.61	27.1	22.8
14.1	32.5	5.97E+00	0.69	3.83	15.8	13.9
14.2	30.2	7.24E+00	0.94	3.16	21.5	22.3
15	56	3.54E+00	0.62	4.00	8.8	7.3
16	66	3.00E+00	1.84	3.36	18.5	15.5
19	6.7	2.86E+01	0.12	3.67	12.6	11.9
Median					9.7	12.4

TABLE 6
Administered Doses and Toxicity

Patient no.	Dose level (GBq/m^2)	Administered activity (GBq)	Weight (kg)	Administered activity (MBq/kg)	Platelet nadir ($\times 10^9$/L)	WBC nadir ($\times 10^9$/L)
1	0.74	1.27	70.0	18.1	199	10.1
2	0.74	1.18	56.0	21.1	321	7.5
3	1.11	2.06	59.0	34.9	52	1.8
4	1.11	1.98	64.0	30.9	183	7.4
6	1.11	2.08	71.0	29.3	143	5.2
7	1.48	2.76	73.0	37.8	277	10.6
8	1.48	2.68	60.0	44.7	89	3.0
9	1.48	2.40	61.5	39.0	202	4.9
10	1.85	3.38	72.0	47.0	89	3.4
11.1	1.85	3.12	64.0	48.7	122	4.5
12.1	1.85	3.34	65.0	51.5	117	2.3
13	2.22	3.61	59.0	61.1	25	0.7
14.1	2.22	3.82	79.0	48.4	78	2.7
15	2.22	4.00	61.0	65.6	47	2.0
16	2.22	3.36	50.0	67.3	18	1.2
17	2.22	3.61	60.0	60.2	12	0.4
18	1.85	3.22	58.0	55.4	8	0.9
19	1.85	3.67	70.0	52.4	94	2.3
20	1.85	2.57	43.5	59.1	65	2.9

The absorbed dose to the red marrow was calculated using the pharmacokinetic data. Because pharmacokinetic data did not vary much between patients (*12*), the interindividual variation in red marrow doses per administered megabecquerel was small as well. There are some factors associated with stable clearance of the mAbs. The antibody is humanized, so aberrant clearance caused by neutralizing antibodies (human antimurine or human antichimeric) is not to be expected. There is no antigenic sink in the bone marrow or other organs influencing clearance of the antibody. Because there is uptake neither in the bone marrow nor in the bone, the main contributor to the red marrow dose is activity in the blood. Therefore, we think it appropriate to use the blood-derived method of Shen et al. to estimate red marrow dose (*11*).

The absorbed red marrow dose correlated well with the blood cell nadirs ($r = -0.69$ for platelets, $r = -0.72$ for WBC). The whole-body dose even showed a slightly better correlation ($r = -0.69$ for platelets, $r = -0.75$ for WBC). Surprisingly, both dosimetry-independent parameters, the administered activity per kilogram of body weight ($r = -0.79$) and the administered activity per square meter of body surface area ($r = -0.73$), correlated well with the blood cell nadirs. The reason to correlate parameters such as dose/kg or absorbed whole-body dose with toxicity is that there are as many administration and dosing schemes as there are RIT trials. Most RIT trials concern the treatment of non-Hodgkin's lymphoma patients. Although trials on patients with this disease cannot be compared with trials on patients with head and neck cancer (differences in pretreatment, intrinsic activity of the mAbs used, localization of disease in the bone marrow, use of murine mAbs), the method of dosing the activity can be discussed. The 2 main dosing schemes are dosimetry based or weight based. The first method uses a tracer dose of ^{131}I-labeled mAb to determine the therapeutic dosage of radioiodinated anti-CD20 mAb tositumomab that would lead to a whole-body dose of 0.75 Gy (*15*). The second method uses a body weight-derived dosing scheme for the ^{90}Y-labeled anti-CD20 mAb ibritumomab (15 MBq/kg) and does not analyze dosimetric data before treatment (*16*). In retrospect, we can consider the suitability of these alternative methods of dosing if they had been applied in the present study. If a dose of 55 MBq/kg (the lowest dose at which grade 4 hematologic toxicity was observed) had been defined as MTD, only 3 patients would have appeared to tolerate a dose of more than 55 MBq/kg without having grade 4 hematologic toxicity (Table 6). Two of them had grade 3 toxicity. If a 0.84-Gy whole-body dose (the lowest whole-body dose at which grade 4 hematologic toxicity was observed) had been chosen as MTD, 9 patients would have been undertreated, since they appeared to tolerate higher whole-body doses. Our data suggest that to dose using the patient's weight can be safe and has the lowest chance of undertreating patients.

The absorbed doses in the tumors tend to vary enormously. These doses were similar to those achieved by treatment with the other anti-CD44v6 conjugate, ^{186}Re-U36 (*4*). The absorbed dose is higher in small lesions than in larger tumors. Although it is to be expected that the smallest tumors will have the highest doses, the actual doses in these tumors could be lower: The statistical error could be significant, because the number of pixels in such a small ROI is low. In the estimation of tumor doses, the influence of necrosis within a tumor is not considered. Radiolabeled antibodies can reach only viable tumor cells, since there are no blood vessels in necrotic parts of the tumor. Moreover, intratumoral pressure plays a more important role in large

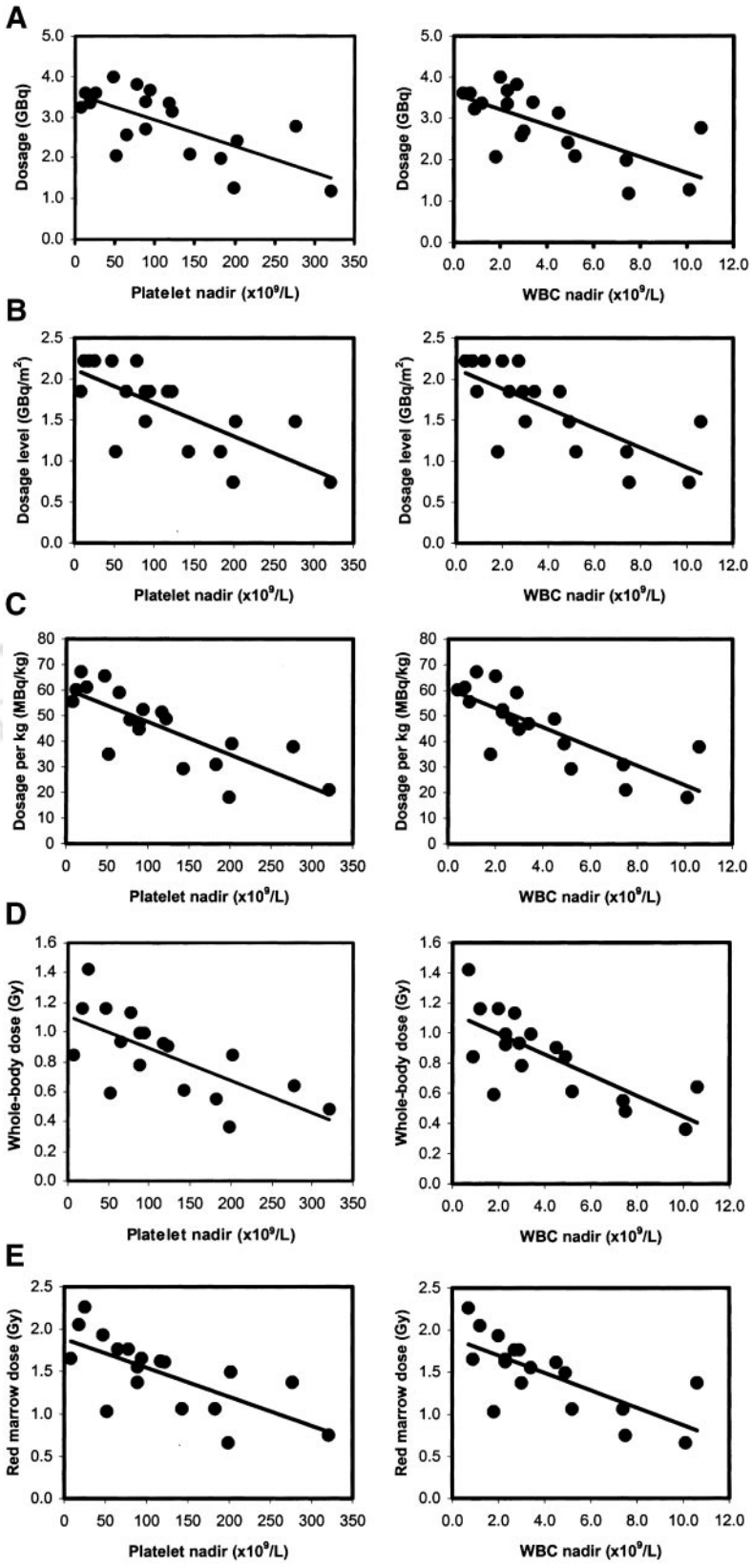

FIGURE 2. Correlation of platelet and WBC nadirs with total injected activity (A), injected activity per square meter of body surface area (B), injected activity per kilogram of body weight (C), whole-body absorbed dose (D), and red marrow absorbed dose (E).

TABLE 7
Correlation Coefficients of Hematologic Toxicity Versus Dose

Parameter	Platelet nadir	WBC nadir
Dose (GBq)	−0.69	−0.69
Dose level (GBq/m^2)	−0.73	−0.73
Dose per kilogram (MBq/kg)	−0.79	−0.79
Whole-body dose (Gy)	−0.69	−0.75
Red marrow dose (Gy)	−0.69	−0.72

lesions. The absorbed dose in the tumor could therefore be estimated more precisely by dividing the absorbed energy through the weight of viable tissue, leading to higher absorbed doses. The fact that high tumor doses can be achieved encourages the thought that ^{186}Re-bivatuzumab can be an effective systemic adjuvant treatment for patients with head and neck cancer with minimal residual disease.

CONCLUSION

Dosimetric analysis of the data on treatment of patients with ^{186}Re-bivatuzumab revealed that the range of doses to normal organs seems to be well within acceptable and safe limits. Attention should be paid to the absorbed dose in the testes. Hematologic toxicity was dose limiting. The administered activity per kilogram of body weight correlated best with the extent of hematologic toxicity. Doses absorbed in tumors were quite similar to those achieved by treatment with the other anti-CD44v6 conjugate, ^{186}Re-U36. Given the acceptable tumor doses, ^{186}Re-labeled bivatuzumab could be a good candidate for future adjuvant RIT in patients with minimal residual disease.

ACKNOWLEDGMENTS

The authors thank Michel de Groot for processing the scintigraphic data and helping with the dosimetric analysis. This study was sponsored by Boehringer Ingelheim BV.

REFERENCES

1. Parkin DM, Bray F, Ferlay J, Pisani P. Estimating the world cancer burden: Globocan 2000. *Int J Cancer.* 2001;94:153–156.
2. Postema EJ, Boerman OC, Oyen WJG, Raemaekers JMM, Corstens FHM. Radioimmunotherapy of B-cell non-Hodgkin's lymphoma. *Eur J Nucl Med.* 2001;28:1725–1735.
3. Heider KH, Sproll M, Susani S, et al. Characterization of a high-affinity monoclonal antibody specific for CD44v6 as candidate for immunotherapy of squamous cell carcinomas. *Cancer Immunol Immunother.* 1996;43:245–253.
4. Colnot DR, Quak JJ, Roos JC, et al. Phase I therapy study of ^{186}Re-labeled chimeric monoclonal antibody U36 in patients with squamous cell carcinoma of the head and neck. *J Nucl Med.* 2000;41:1999–2010.
5. Coover LR, Silberstein EB, Kuhn PJ, Graves MW. Therapeutic ^{131}I in outpatients: a simplified method conforming to the Code of Federal Regulations, title 10, part 35.75. *J Nucl Med.* 2000;41:1868–1875.
6. Siegel JA, Kroll S, Regan D, Kaminski MS, Wahl RL. A practical methodology for patient release after tositumomab and ^{131}I-tositumomab therapy. *J Nucl Med.* 2002;43:354–363.
7. Visser GWM, Gerretsen M, Herscheid JDM, Snow GB, van Dongen GAMS. Labeling of monoclonal antibodies with rhenium-186 using the MAG3 chelate for radioimmunotherapy of cancer: a technical protocol. *J Nucl Med.* 1993;34: 1953–1963.
8. Buijs WCAM, Oyen WJG, Dams ETM, et al. Dynamic distribution and dosimetric evaluation of human non-specific immunoglobulin G labelled with ^{111}In or ^{99m}Tc. *Nucl Med Commun.* 1998;19:743–751.
9. Buijs WCAM, Siegel JA, Boerman OC, Corstens FHM. Absolute organ activity estimated by five different methods of background correction. *J Nucl Med.* 1998;39:2167–2172.
10. Stabin MG. MIRDOSE: personal computer software for internal dose assessment in nuclear medicine. *J Nucl Med.* 1996;37:538–546.
11. Shen S, DeNardo GL, Sgouros G, O'Donnell RT, DeNardo SJ. Practical determination of patient-specific marrow dose using radioactivity concentration in blood and body. *J Nucl Med.* 1999;40:2102–2106.
12. Börjesson PKE, Postema EJ, Roos JC, et al. Phase I therapy study with ^{186}Re-labeled humanized monoclonal antibody BIWA 4 (bivatuzumab) in patients with head and neck squamous cell carcinoma. *Clin Cancer Res.* 2003. In press.
13. Paganelli G, Zoboli S, Cremonesi M, et al. Receptor-mediated radiotherapy with ^{90}Y-DOTA-D-Phe1-Tyr3-octreotide. *Eur J Nucl Med.* 2001;28:426–434.
14. Press OW, Eary JF, Appelbaum FR, et al. Radiolabeled-antibody therapy of B-cell lymphoma with autologous bone marrow support. *N Engl J Med.* 1993; 329:1219–1224.
15. Wahl RL, Kroll S, Zasadny KR. Patient-specific whole-body dosimetry: principles and a simplified method for clinical implementation. *J Nucl Med.* 1998; 39(suppl):14S–20S.
16. Wagner HN Jr, Wiseman GA, Marcus CS, et al. Administration guidelines for radioimmunotherapy of non-Hodgkin's lymphoma with ^{90}Y-labeled anti-CD20 monoclonal antibody. *J Nucl Med.* 2002;43:267–272.